09

Study of angular and temperature dependences of Cr^{3+} impurity luminescence in β-Ga_2O_3

© V.Yu. Davydov[1], Yu.E. Kitaev[1], N.S. Averkiev[1], A.N. Smirnov[1], I.A. Eliseyev[1], D.K. Nelson[2], D.I. Panov[2], V.A. Spiridonov[2], D.A. Bauman[2], A.E. Romanov[2,1]

[1] Ioffe Institute,
St. Petersburg, Russia
[2] ITMO University,
St. Petersburg, Russia

E-mail: valery.davydov@mail.ioffe.ru

Received April 30, 2024
Revised October 28, 2024
Accepted October 30, 2024

Using the combination of angle-resolved spectroscopy and symmetry analysis of the Cr^{3+} ion levels in the β-Ga_2O_3 matrix, the features of luminescence of Cr^{3+} impurity in monoclinic β-Ga_2O_3 doped with Cr were studied. For the first time, angular dependences of the intensities of the R_1 and R_2 Cr^{3+} lines were experimentally obtained and analyzed theoretically for three crystallographic planes (100), (010), and (001). For the first time, in the spectra of β-Ga_2O_3:Cr, two lines R_3 and R_4, which were not observed earlier, were detected. The nature of these lines was analyzed within the model of $Cr^{3+}-Cr^{3+}$ pair defects.

Keywords: β-Ga_2O_3, Cr^{3+} impurity, photoluminescence, symmetry analysis.

DOI: 10.61011/PSS.2024.12.60197.6594PA

Due to its high transparency, a wide-band semiconductor β-Ga_2O_3 is a good matrix for optically active centers radiating in the spectral region stretching from the near UV to the near IR ranges. In particular, doping Cr^{3+} provides for effective irradiation in the red region, which is caused by internal transitions in an impurity ion [1,2]. With this consideration in mind, β-Ga_2O_3:Cr demonstrates a great potential of use in ionizing radiation detectors [3,4]. It is also promising to research the live organisms, since the irradiation is located in the so called first window (700−950 nm), where the biological tissue has the absorption minimum [5]. The objective of this paper was to obtain new information using experimental and theoretical methods on the features the Cr^{3+} impurity luminescence in the β-Ga_2O_3 matrix in the wide temperature range.

Chromium-doped bulk crystals β-Ga_2O_3 grown by Czochralski method in ITMO were studied [6]. The vibrational and electronic characteristics of crystals by micro-Raman light scattering (μ-RS) and micro-photoluminescence (μ-PL) were measured using a LabRAM HREvo UV-VIS-NIR-Open spectrometer (Horiba, France). To excite μ-RS and μ-PL spectra, Nd:YAG laser line $\lambda = 532$ nm (2.33 eV) was used. μ-PL spectra with angular resolution were measured in the temperature range of (10−300 K).

μ-PL spectrum of β-Ga_2O_3:Cr presented in Figure 1, *a* demonstrates two sharp peaks R_1 and R_2, wavelengths of which at $T = 80$ K are equal to 695.5 nm (1.783 eV) and 688.4 nm (1.801 eV) accordingly. Their origin, as it was established by the selection rules [4], is related to $^2E_g \rightarrow {}^4A_{2g}$ transitions in Cr^{3+} ion with octahedral environment of oxygen atoms. The same figure presents angular dependences of intensities of R_1 and R_2 lines of monoclinic β-Ga_2O_3:Cr^{3+} for three crystallographic planes (100), (010) and (001), which were first experimentally obtained within this study.

To interpret experimental data, the theoretical group analysis produced the selection rules for the permitted polarizations of optical transitions in various geometries of the experiment. To determine the selection rules in the photoluminescence spectra of impurity ions in the crystals, it is necessary to set the crystal structure (i.e. its space group and placement of atoms in the symmetry positions — Wyckoff positions) and local symmetry of the impurity. The β-phase of crystal Ga_2O_3 that we study belongs to the monoclinic system, and its symmetry is described by the space group $C2/m$ with the 2-fold symmetry axis directed along the translation vector **b** (Figure 1, *b*). Vector **b** [010] is perpendicular to plane ac, i.e. the crystalline face (010). Translation vectors **a** and **c**, the angle of which is 103.83°, are directed along crystallographic directions [100] and [001] accordingly and do not match with Cartesian axes x and z.

In β-phase of crystal Ga_2O_3 there are two non-equivalent orbits Ga1 and Ga2, each comprising 4 Ga atoms. At the same time each of Ga atoms of both orbits has the same local symmetry described by a point group $C_s = \{m_{010}|0\}$, comprising mirror plane of symmetry m, perpendicular to the 2-fold axis of symmetry. Gallium atoms of the first Ga1 orbit have tetrahedral environment of oxygen atoms, and of the second Ga2 orbit — the octahedral one. Cr^{3+} ions, as was shown in paper [7], substitute Ga2 atoms with the octahedral environment.

In articles [8,9] the classification of Cr^{3+} ion states in β-phase of Ga_2O_3 crystal is given on the basis of the irreducible representations of the local cubic group O_h, and not

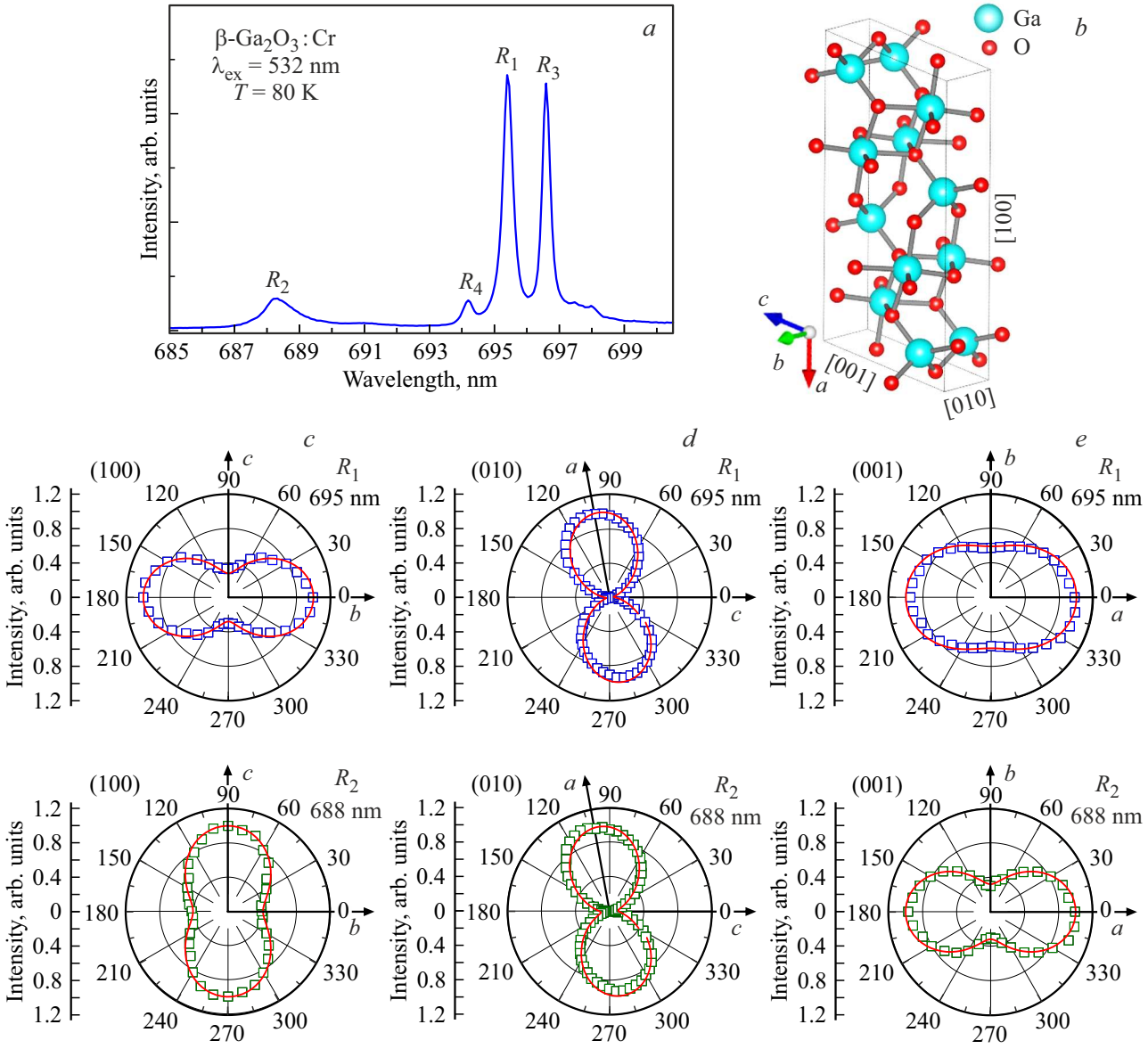

Figure 1. *a* — PL spectrum of β-Ga_2O_3:Cr, registered from plane (100); *b* — crystalline structure β-Ga_2O_3; *c*–*e* — dependences of intensity of PL lines R_1 and R_2 β-Ga_2O_3, registered from planes (100) (*c*), (010) (*d*) and (001) (*e*), as functions of the angle between the direction of the polarization vector **E** and crystallographic axes.

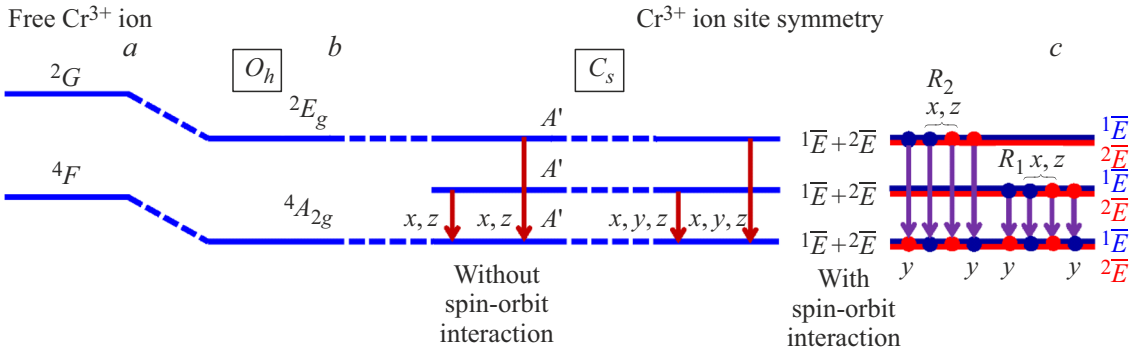

Figure 2. Evolution of electron states of chromium ion Cr^{3+}: *a* — free ion; *b* — single ion with octahedral environment of oxygen atoms in the field with symmetry O_h; *c* — single ion Cr^{3+}, which occupies in the β-Ga_2O_3 matrix the Ga position with local symmetry C_s.

C_s, at the same time the symmetry of states with account of the spin-orbit interaction on the basis of the irreducible representations of the double groups is not given at all.

In the local field with symmetry C_s the levels ^2E_g and $^4A_{2g}$ of ion Cr^{3+} in the octahedral environment transform into $2A'$ and A' accordingly, and with account of spin-orbit interaction each of the three levels transform into twofold degenerate state $^1\overline{E} + {}^2\overline{E}$, the symmetry of which is described by two complex-conjugate two-digit irreducible representations. In case of presence of even very weak magnetic field, the degeneracy is removed, and $^1\overline{E}$ and $^2\overline{E}$ states become independent. In Figure 2 these states are shown with different colors.

The selection rules for the allowed polarizations of transitions between the initial D^i and final D^f electron states are determined by the following conditions:

– between the states with the same symmetry, transitions in polarization x, z are allowed

$$(^1\overline{E})^* x\, ^1\overline{E} = (^2\overline{E})^* x\, ^2\overline{E} = A'(x, z),$$

– between the states with the different symmetry, transitions in polarization y are allowed

$$(^1\overline{E})^* x\, ^2\overline{E} = (^2\overline{E})^* x\, ^1\overline{E} = A''(y).$$

Based on the obtained selection rules, one can determine the space diagrams of SiC intensity distribution for each of the allowed transitions.

Let us consider the three available geometries of the experiment corresponding to the different planes of PL polarization (100), (010) and (001), each demonstrating two luminescence lines R_1 and R_2 (see Figure 1, *c–e*).

For plane (100), the results of PL angular dependence for which are shown in Figure 1, *c*, polarization vector **E** has components along axes y and z and is a superposition of the fields of two transitions that are incoherent to each other, since they are related to the transitions between different states. In this case the angular dependence of $I(\varphi)$ PL intensity in y, z plane, where the direction, in which the intensity is measured, is set by angle φ, counted from axis y, and has the following appearance: $I(\varphi) = E_z^2 \cos^2\varphi + E_y^2 \sin^2\varphi$. Modeling of experimental results presented in Figure 1, *c*, leads to the conclusion that for R_1 and R_2 lines the ratios of modules E_z and Ey differs: for line R_1 $E_z < E_y$, and for line R_2 $E_z > E_y$.

For plane (010), the results of PL angular dependence for which are shown in Figure 1, *d*, each R_1 and R_2 PL line may be contributed by two transitions ($^1\overline{E} \to {}^1\overline{E}$ and ($^2\overline{E} \to {}^2\overline{E}$, authorized in polarizations x, z (i. e. in the plane determined by vectors **a** and **c**). According to the above selection rules, in this case for each transition the polarization vector **E** has the components along axes x and z, $\mathbf{E_x} = E_x \mathbf{e_x}$ and $\mathbf{E_z} = E_z \mathbf{e_z}$, which are coherent, since are related to one and the same transition. Direction of vector **E** in plane ac is set by angle ψ, where $\mathrm{tg}\,\psi' = E_z'/E_x'$ ($\mathrm{tg}\,\psi'' = E_z''/E_x''$, and the direction along which PL intensity $I(\varphi)$ is measured — by angle φ. It is important to note that E_z/E_x ratio may differ significantly for lines R_1 and R_2, and for transitions $^1\overline{E} \to {}^1\overline{E}$ and $^2\overline{E} \to {}^2\overline{E}$, which contribute to one and the same line. In the general case the angular dependence of luminescence intensity, being a superposition of intensities of both transitions $^1\overline{E} \to {}^1\overline{E}$ and $^2\overline{E} \to {}^2\overline{E}$, in the plane ac should look as follows

$$I(\varphi) = (E_x'^2 + E_z'^2)\cos^2(\varphi - \psi') + (E_x''^2 + E_z''^2)\cos^2(\varphi - \psi'').$$

Using angular dependences of luminescence (Figure 1, *d*) we can determine the ratios of amplitudes E_z'/E_x' and E_z''/E_x'' for transitions $^1\overline{E} \to {}^1\overline{E}$ and $^2\overline{E} \to {}^2\overline{E}$ for each of the lines R_1 and R_2. Modeling of experimental results presented in Figure 1, *e*, leads to the conclusion that transitions $^1\overline{E} \to {}^1\overline{E}$ and $^2\overline{E} \to {}^2\overline{E}$ are approximately same in intensity, and in both cases modules are $E_x > E_z$. However, the directions of irradiation polarization for every transition differ, and the angle between them is 40–65°.

For plane (001), the results of PL angular dependence for which are shown in Figure 1, *e*, polarization vector **E** has the components along axes y and x. Same as in the geometry case (100), it is a superposition of the fields of two transitions that are incoherent to each other, since they are related to the transitions between different states. In this case the angular dependence of luminescence in plane y, x looks as follows $I(\varphi) = E_x^2 \cos^2\varphi + E_y^2 \sin^2\varphi$, where angle φ counts from axis x. Modeling of experimental results given in Figure 1, *e*, leads to the conclusion that for both lines R_1 and R_2 the modules are $E_x > E_y$.

Summarizing all the above, one can conclude that the ratio of modules of values E_i for various lines is different. For R_1 this ratio is: $E_x > E_z$, $E_x > E_y$ and $E_z < E_y$; and for R_2 it is different: $E_x > E_z$, $E_x > E_y$ and $E_z > E_y$. Since values E_i are related to the view of the basic functions of

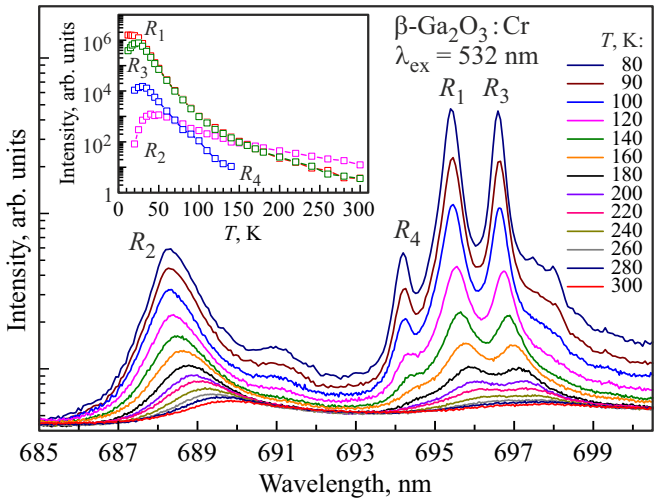

Figure 3. PL spectra β-Ga_2O_3:Cr in temperature range 80–300 K. The spectra were registered from plane (100). The insert shows dependence of intensity of lines R_1, R_2, R_3 and R_4 in the temperature range of 10–300K. All data are presented in semilogarithmic scale.

irreducible representations of group C_s, the prevalence of E_x means that wave functions of the defect are formed of orbits oriented along axis x. These data may be useful to identify other transitions, if they are close in their energy to lines R_1 and R_2, and to build a microscopic model of defect (Cr) providing these lines.

Apart from R_1 and R_2 lines, for the first time PL spectra β-Ga_2O_3:Cr show two new sharp peaks R_3 and R_4, wavelengths of which at $T = 80\,\mathrm{K}$ are equal to 696.7 nm (1.780 eV) and 694.3 nm (1.786 eV) accordingly (Figure 1, *a*). Study of the angular dependence of their intensity made it possible to establish that both these lines are observed only in plane (100), have linear polarization, matching the direction of the crystallographic axis from monoclinic β-Ga_2O_3 and are characterized by unusual temperature dependences (Figure 3).

To interpret these results, we proposed a model of paired $Cr^{3+}-Cr^{3+}$ defects. The orbit with octahedral environment of Ga2 atoms with oxygen atoms together with single ions Cr^{3+}, replacing one of Ga2 atoms, also has pairs of ions Cr^{3+}, replacing Ga2 atoms. This pair defect with the center in the origin of coordinates (000) may be considered as a system having its own symmetry. Its local symmetry is described by a point group C_{2h}. Within this model, a system of energy levels was specified for this pair and the selection rules for the allowed PL polarizations of such pairs. It was found that in case of a pair defect, without the spin-orbit interaction, the irradiation with polarization along the direction of the second order axis $b(y)$ is prohibited by the selection rules. Irradiation with polarizations along axes x and z is permitted. Based on this approach, it was possible to interpret the polarization dependences obtained in the experiment. Results of the analysis of the temperature dependences of allowed PL parameters in lines R_3 and R_4 will be presented in the detailed publication.

Funding

The studies were partially supported within the state assignments of the Ministry of Science and Higher Education, Ioffe Institute (FFUG-2024-0018 and FFUG-2024-0043) and the Russian Science Foundation (project No. 24-12-00229).

Conflict of interest

The authors declare that they have no conflict of interest.

References

[1] H.H. Tippins. Phys. Rev., **137**, A865 (1965). DOI: 10.1103/PhysRev.137.A865
[2] E. Nogales, J.A. Garcia, B. Mendez, J. Piqueras. J. Appl. Phys., **101**, 33517 (2007). DOI: 10.1063/1.2434834
[3] M. Peres, D.M. Esteves, B.M.S. Teixeira, J. Zanoni, L.C. Alves, E. Alves, L.F. Santos, X. Biquard, Z. Jia, W. Mu, J. Rodrigues, N.A. Sobolev, M.R. Correia, T. Monteiro, N. Ben Sedrine, K. Lorenz. Appl. Phys. Lett., **120**, 261904 (2022). DOI: 10.1063/5.0089541
[4] V.Yu. Davydov, A.N. Smirnov, I.A. Eliseev, Yu.E. Kitaev, Sh.Sh. Sharofidinov, A.A. Lebedev, D.Yu. Panov, V.A. Spiridonov, D.A. Bauman, A.E. Romanov, V.V. Kozlovsky. FTP, **56**, 573 (2023). (in Russian). https://doi.org/10.61011/FTP.2023.07.56794.5202C
[5] E. Hemmer, A. Benayas, F. Legare, F. Vetrone. Nanoscale Horiz., **1**, 168 (2016). DOI: https://doi.org/10.1039/C5NH00073D
[6] D.A. Bauman, D.I. Panov, D.A. Zakgeim, V.A. Spiridonov, A.V. Kremleva, A.A. Petrenko, P.N. Brunkov, N.D. Prasolov, A.V. Nashchekin, A.M. Smirnov, M.A. Odnoblyudov, V.E. Bougrov, A.E. Romanov. Phys. Status. Solidi A, **218**, 2100335 (2021). DOI:10.1002/pssa.202100335
[7] S. Sugano, Y. Tanabe. J. Phys. Soc. Japan, **13**, 880 (1958). DOI: 10.1143/JPSJ.13.880
[8] A. Fiedler, Z. Galazka, K. Irmscher. J. Appl. Phys., **126**, 213104 (2019). DOI: 10.1063/1.5125774
[9] J.E. Stehr, M. Jansson, D.M. Hofmann, J. Kim, S.J. Pearton, W.M. Chen, I.A. Buyanova. Appl. Phys. Lett., **119**, 052101 (2021). DOI: 10.1063/5.0060628

Translated by M.Verenikina